# Experimental Results of a Compressive Reflector Antenna Producing Spatial Coding

Ali Molaei\*, Katherine Graham\*, Luis Tirado\*, Ashkan Ghanbarzadeh<sup>†</sup>, Anthony Bisulco\*, Juan Heredia-Juesas\*<sup>†</sup>,
Chang Liu<sup>†</sup>, Joseph Von Holten<sup>‡</sup>, Jose A. Martinez-Lorenzo\*<sup>†</sup>

\*Electrical & Computer Engineering, Northeastern University, Boston, MA, USA

<sup>†</sup>Mechanical & Industrial Engineering, Northeastern University, Boston, MA, USA

<sup>‡</sup>Chemical Engineering, Northeastern University, Boston, MA, USA

Abstract—This paper presents the design and fabrication of a Compressive Reflector Antenna (CRA) for high-sensing-capacity millimeter-wave imaging applications. The CRA is fabricated using additive manufacturing or 3D printing and metalized by applying silver conductive coating spray on its surface. The nearfields of the CRA are measured when it is fed by a conical horn antenna, a compressive horn antenna, and a perturbed cavity. The singular value distribution and sensing capacity of the CRA fed by the aforementioned antennas are calculated and compared.

### I. Introduction

Millimeter-wave (mm-wave) sensing systems are used in several near-field imaging applications, such as security screening, non-destructive testing, autonomous driving, and elsewhere [1]–[3]. Recently, there has been a great interest in electronically-scanned antennas for such systems, due to their fast (real-time) beamforming capabilities. However, such systems usually require active components to perform the beamforming, adding cost and hardware complexity to the system.

Compressive imaging enables different hardware platforms to overcome some of the drawbacks caused by the traditional electronically-scanned antennas [4], [5]. A Compressive Reflector Antenna (CRA) [5], for example, has the capability to create spatial and spectral codes in the near- and far-field of the antenna, making it a good substitute for traditional electronically-scanned antennas.

This paper presents our preliminary results on the design and experimental validation of a CRA that it is fed with a conical horn antenna, a Compressive Horn Antenna (CHA), and a perturbed cavity. The measured near-fields of the CRA, when excited by the aforementioned feeds, and their associated sensing capacities are presented and compared.

# II. FABRICATION OF THE CRA

A CRA is a doubly-curved offset parabolic reflector antenna, whose surface is tailored by specially designed scatterers—see [5] for a detailed description on the design of the CRA. The CRA has the capability to create pseudorandom spatial and spectral codes in the near- and far-field of the antenna, making it a good candidate for high-sensing-capacity imaging applications.

The CRA presented here is manufactured by introducing PEC scatterers on the surface of the reflector. The geometrical

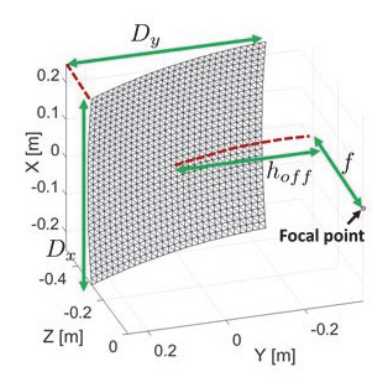


Fig. 1. Geometry of the proposed CRA in an offset configuration.

configuration and design parameters of the CRA studied in this paper are presented in Fig. 1 and Table I, respectively. The CRA is fabricated using additive manufacturing or 3D printing. Due to the print size limitations of the printer, the geometry of the CRA was printed into 9 pieces and assembled afterwards. The surface of the printed parts were metalized using an acrylic-based silver conductive coating spray (842ARSUPER SHIELD  $^{TM}$ ). Figure 2 shows the metalized CRA mounted on the experimental setup for measuring the near-field on a 2D aperture.

TABLE I
DESIGN PARAMETERS FOR THE CRA.

PARAMETER	VAL.	PARAMETER	VAL.
Aperture size $(D_x = D_y)$	50 cm	Size of the rand. facets	$4\lambda$
Focal length $(f)$	50~cm	Max. Distortion of facets	3°
Offset height $(h_{off})$	35~cm		

### III. NEAR-FIELD MEASUREMENT

The performance of the fabricated CRA is evaluated by measuring the near-field of the antenna and calculating its Singular Value (SV) distribution and sensing capacity. For this purpose, the reflector is fed with three different antenna elements: (1) A 3D printed conical horn with diameter of 21 mm and length of 40 mm (Fig. 3(a)); (2) a Compressive Horn Antenna (CHA), which is composed of a plastic with pseudo-random shape slid inside a pyramidal horn antenna

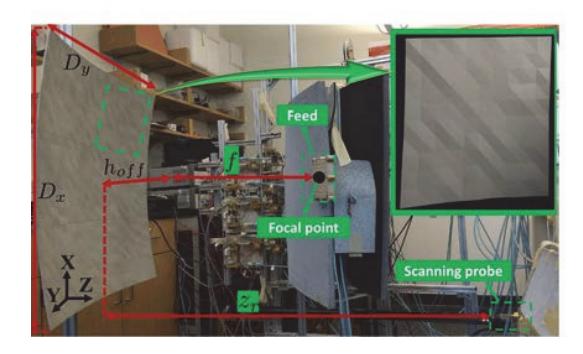


Fig. 2. Experimental setup: The CRA is positioned  $z_r=90\ {\rm cm}$  far from a scanning tapered WR-12 probe.

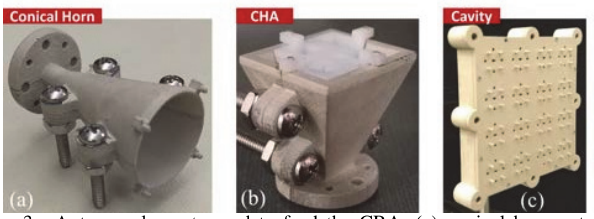


Fig. 3. Antenna elements used to feed the CRA: (a) conical horn antenna, (b) CHA, and (c) perturbed cavity.

(Fig. 3(b))—see [6] for a detailed description on CHA; and (3) a perturbed rectangular cavity with a size of 96 mm×96 mm×21 mm (Fig. 3(c)). A cut section of a metallic sphere of radius 10 mm is attached to one corner of the rectangular cavity to perturb the fields and excite several resonance modes inside of it. The cavity consists of 16 slots on one of the walls of the cavity to sample the cavity modes and illuminate the reflector. Figure 4 shows the magnitude and phase of the electric field, measured at  $z_r = 90$  cm far from the center of the CRA, when it is illuminated by the aforementioned feeding elements. It can be inferred from these plots that the perturbed cavity provides more randomness in the radiated fields (spatial codes) than the other two feeding elements.

The sensing matrix  $\bf A$  of the CRA-based imaging system is defined as the Gramian matrix of the measured electric fields  $\bf E$  in the near-field region of the antenna, and it is obtained as follows:  $\bf A = \bf E^t \bf E$ . Figure 5(a) shows an improved SV distribution for the CRA fed by the perturbed cavity antenna over the other two types of feeding antennas. This means that the cavity is providing a relatively flatter SV spectrum. Figure 5(b) shows the sensing capacity of the CRA system provided in [5], which is defined as the maximum amount of information that can be transferred through an imaging system. The reduced spill-over of the conical horn antenna leads to a better signal to noise ratio and an enhanced capacity plot. Nevertheless, all of them provide significant spatial coding.

### IV. CONCLUSION

This paper presents the near-field measurement results of a CRA, designed for high-sensing-capacity imaging applications. The SV distribution and sensing capacity of the CRA is calculated for different feeding elements. The CRA and the feeding antennas are fabricated using 3D printing; and, then,

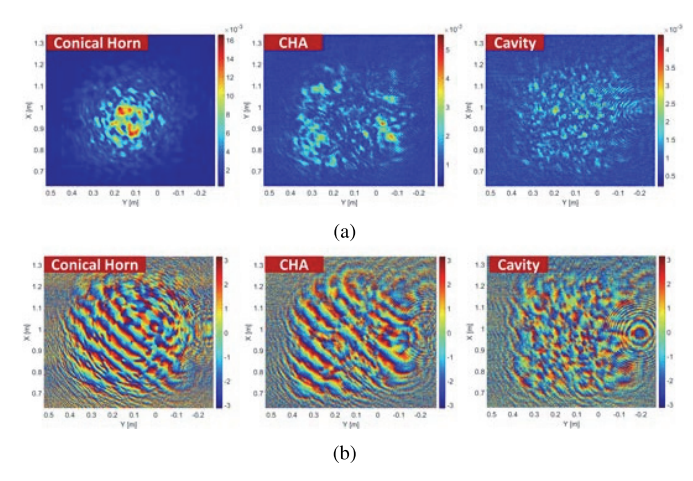


Fig. 4. (a) Magnitude and (b) Phase of the electric field measured at  $z_r = 90$  cm far from the center of the CRA.

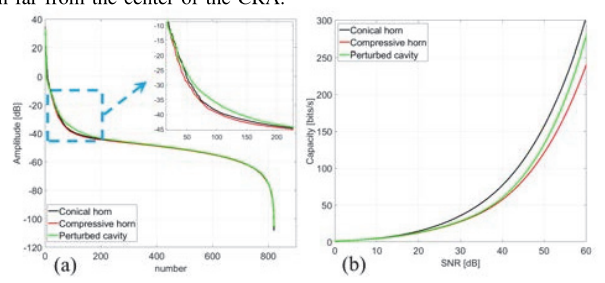


Fig. 5. (a) SV distribution and (b) Sensing capacity of the CRA fed by different antenna elements.

they are metalized using a conductive silver spray. This method highly reduces the fabrication cost of the system, compared to the tradition fabrication techniques.

## **ACKNOWLEDGEMENT**

This work has been partially funded by the NSF CAREER program (Award No. 1653671) and the U.S. Department of Homeland Security (Award No. 2013-ST-061-ED0001).

### REFERENCES

- S. Kharkovsky and R. Zoughi, "Microwave and millimeter wave nondestructive testing and evaluation-overview and recent advances," *IEEE Instrumentation & Measurement Magazine*, vol. 10, no. 2, pp. 26–38, 2007
- [2] A. Jam and K. Sarabandi, "A horizontally polarized beam-steerable antenna for sub-millimeter-wave polarimetric imaging and collision avoidance radars," in *Antennas and Propagation (APSURSI)*, 2016 IEEE International Symposium on. IEEE, 2016, pp. 789–790.
- [3] D. Sheen, D. McMakin, and T. Hall, "Three-dimensional millimeter-wave imaging for concealed weapon detection," *Microwave Theory and Techniques, IEEE Transactions on*, vol. 49, no. 9, pp. 1581–1592, 2001.
- [4] D. R. Smith, M. S. Reynolds, J. N. Gollub, D. L. Marks, M. F. Imani, O. Yurduseven, D. Arnitz, A. Pedross-Engel, T. Sleasman, P. Trofatter et al., "Security screening via computational imaging using frequency-diverse metasurface apertures," in *Passive and Active Millimeter-Wave Imaging XX*, vol. 10189. International Society for Optics and Photonics, 2017, p. 101890B.
- [5] A. Molaei, J. H. Juesas, and J. A. M. Lorenzo, "Compressive reflector antenna phased array," in *Antenna Arrays and Beam-formation*. InTech, 2017
- [6] A. Molaei, J. Heredia-Juesas, L. Tirado, A. Zhang, Weite Bisulco, A. Zhu, D. Cachay, A. Ghanbarzadeh, and J. Martinez-Lorenzo, "3d printed compressive horn antenna for high-sensing-capacity millimeterwave imaging," in *Antennas and Propagation (EUCAP)*, 2018 12th European Conference on. IEEE, 2018.